Papadopoulos, S., & Sextos, A. (2018). Anti-symmetric mode excitation and seismic response of base-isolated bridges under asynchronous input motion. *Soil Dynamics and Earthquake Engineering*, *113*, 148-161. https://doi.org/10.1016/j.soildyn.2018.06.004

Anti-symmetric mode excitation and seismic response of base-isolated bridges under asynchronous input motion

Savvas P. Papadopoulos [a], Anastasios G. Sextos [b]

[a] Civil Engineer, MSc, Ph.D. Candidate, Division of Structural Engineering, Department of Civil Engineering, Aristotle University Thessaloniki, Greece; e-mail: savvaspp@civil.auth.gr

[b] Associate Professor, Division of Structural Engineering, Department of Civil Engineering, Aristotle University Thessaloniki, Greece, tel.; e-mail: asextos@civil.auth.gr and Department of Civil Engineering, University of Bristol, UK (a.sextos@bristol.ac.uk) (*Corresponding Author)

ABSTRACT

This paper investigates the effect of asynchronous earthquake ground motion on the transverse response of base-isolated bridges. In this context, the excitation of anti-symmetric modes of vibration under asynchronous input is examined and is statistically correlated with characteristic engineering demand parameters. Different ground motion scenarios are considered for various combinations of soil class, wave propagation velocity and loss of correlation patterns among different support motions, using a spectral representation method to generate m-variate, fully non-stationary, EC8 spectrum-compatible ground motion vector processes. It is shown that in the idealised case of the wave passage effect only, the detrimental effects of asynchronous excitation are concentrated on the very last piers along the direction of the seismic waves. However, when loss of coherency is also taken into account in a more realistic scenario, the impact of spatial variability is significantly more uniformly distributed. Most importantly, the conditional probability of a detrimental increase in an EDP of interest (i.e., pier base bending moments and deck drift) under multi-support excitation given that an anti-symmetric mode is excited is not only uniform but also considerably high. This is a clear evidence that the local increase of seismic demand in the bridge studied is associated with the excitation of the first anti-symmetric mode of vibration.

Keywords: bridges, multi-support excitation, spatial variability, anti-symmetric modes, spectral representation method, evolutionary power spectrum

INTRODUCTION

During the last decades, the asynchronous excitation of long structures, such as bridges and pipelines, has attracted scientific attention. Past experience from catastrophic earthquakes, available data from dense accelerometric arrays all over the world and the evolution of computational power gave impetus to the systematic study of the spatial variability of earthquake ground motion (SVEGM) and its impact on extended structures. Bridges in particular, have been thoroughly studied both because of their wider socioeconomic importance and the fact that they commonly extend over distances equivalent to the seismic wavelengths or even cross irregular topographies. The result of the latter is that ground motions arriving at bridge supports may vary significantly in terms of arrival time, frequency content and amplitude, thus affecting significantly their seismic performance.

The causes of the SVEGM can generally be summarized in [1]: (a) the wave passage effect, (b) the loss of coherency of the seismic waves as a result of multiple reflections, refractions and superposition within the soil media, (c) the local site effects, and (d) the attenuation of the seismic waves, which, for the dimensions of the bridges usually examined, is not significant. Soil-structure interaction (SSI) has also been identified as an additional source of spatial variation [2] but is mainly accounted for in cases of spatially varying soil profiles or soft soil formations. The above sources of spatial variation of earthquake ground motion are expressed in terms of the signal correlation, which tends to decay with distance and frequency. Based on the records of dense seismograph arrays mainly in Taiwan, Japan and the U.S., the literature has proposed numerous coherency models (e.g. empirical [3–5], semi-empirical [6,7], analytical [8,9] etc.) that can be then used for generating suites of spatially variable motions.

Over the years, different methods have been developed for the computation of structural response under multi-support excitation, each one exhibiting different shortcomings [10]. For example, random vibration techniques and response spectrum oriented methods are not commonly used in practice since they are restricted to linear / linearized problems. On the other hand, simulation of non-synchronous ground motions in time history analysis is a more straightforward option for the calculation of the structural (linear or not) response in a Monte Carlo framework. In this context, numerous simulation techniques have been developed for the generation of spatially variable ground motions; these either describe the random field through the combination of a power spectral density (PSD) model with a coherency one, or they simulate them conditioned to "known" accelerograms [11,12]. Spectral representation is one of the most popular methods for the simulation of random fields [13,14]. Shinozuka [15] used spectral representation to simulate uni-

and multi-variate, multi-dimensional, homogeneous or heterogenous stationary processes. The computational efficiency of the method was improved with the use of the FFT technique in the case of stationary processes [16]. This method has also been further extended to simulate ergodic, multivariate, stochastic processes [17,18] so that different local soil conditions between the generation points [19,20] and multi-dimensional Gaussian stochastic fields' simulation could be considered [21]. Hao et al. [22] presented a method based on covariance decomposition for uniform soil conditions, while Gao et al. [23] extended this method in order to simulate ground motions at sites with different power spectral densities (PSD). Recently, Lavorato et al. [24,25] introduced an approach for the generation of arrays of asynchronous signals at different points in space, starting from natural accelerograms related to a given seismic event in order to increase the number of the available data including soil amplification treatment.

In accordance with modern seismic code provisions, different approaches have been proposed to meet the requirements for response spectrum compatibility of simulated ground motions. Hao et al. [22] presented an iterative process that modifies the Fourier coefficients of the simulated motions until the convergence between the target and the generated response spectra becomes sufficient, while Deodatis [19] introduced an iterative scheme that updates the PSD of the process. Bi & Hao (2012) [20] extended this approach by estimating the initial PSD with respect to the target response spectrum instead of considering an arbitrary one, thus leading to fewer iterations. However, the simulated ground motions produced from the aforementioned processes deviate from the Gaussian distribution and the mean computed coherence differs from the targeted one [26]. To overcome these weaknesses, Shields [26] recently presented a method that updates the evolutionary PSD through random functional perturbations. In addition, the method of Cacciola [27] for the simulation of fully non-stationary, spectrum-compatible earthquake motions at a single point, was extended for the purposes of multi-variate simulation by Cacciola & Deodatis [28]. In this method, spectrum compatibility is satisfied through the superposition of an appropriate corrective quasi-stationary process to a "known" fully non-stationary process that represents the seismological properties of the region. Cacciola & Zentner [29] further extended this method to include the natural variability of relevant ground motion parameters. The advantage of the last two methods lies in the fact that the generated ground motions do not need any iteration in order to match the targeted response spectra which is a major step forward compared to previous time consuming methods.

Given the breadth of available methods for the analysis of structural response under multiple support excitation, several analytical studies have been presented in the literature with the aim to

investigate and quantify the sensitivity of different types and configurations of bridges to non-synchronous seismic input. For instance, random vibration analysis has been used to estimate the response of highway [30,31], suspension [32,33] and cable-stayed bridges [34–36]. The impact of multi-support excitation on the seismic behavior of bridges has also been investigated in the frequency (using response spectrum-based methods [1,37–43]) and the time domain. In the second case, numerous studies investigated both the linear and/or the non-linear response of different types of bridges, namely: (a) straight bridges on uniform [44–47] or varying soil profiles, ignoring [45,47,48] or accounting for the soil-structure interaction (SSI) effects [49,50], (b) curved bridges [47,51,52], (c) skewed bridges [45,53], and (d) isolated bridges [54–57]. An extensive comparative study of 27 different structural bridge systems was presented by Sextos & Kappos [58]. Sensitivity of cable-stayed bridges in terms of SVEGM has been studied analytically [34,59] and based on existing measurements. Sextos et al. [60] presented a study on the Evripos cable-stayed bridge using real, free-field records, as well as respective superstructure recordings obtained during the (M_s=5.9, 1999) Athens earthquake. Soil-structure interaction has been further accounted for a 59-span bridge with several bearing types and irregularity features by Mwafy et al. [61] and Yang et al. [62].

Common theme across the aforementioned studies is the significantly different response of bridges under multi-support excitation. This may vary among different studies, however, in the vast majority of cases researchers agree that it is hard to be captured using uniform input ground motion assumptions. The influence of the SVEGM on the response of different bridge components is of course related to the engineering demand parameters examined and case sensitive to the ground motion scenario considered, a fact that hinders a realistic estimate of the SVEGM impact in advance and limits the application of deterministic schemes. As a result, naturally, the problem has gradually started being studied in a probabilistic manner.

A second general observation that the researchers tend to agree, in principle, is that when the loss of coherency to the spatially variable motions is minor or not considered in the formulation, the asynchronous excitation tends to have a favorable effect on the overall dynamic response of bridges. This is a convenient outcome, though only applicable in the rare case of uniform soil profiles along the bridge length, where the rate of coherency decay with distance is very mild due to limited reflections and refractions of seismic waves. In this case, the wave passage effect is dominant and effects of spatial variability can be neglected. In the majority of cases, however, the problem remains multi-parametric and quite unpredictable.

Nevertheless, there is one important observation that has not been thoroughly and systematically studied even though it has been made in several cases [33,42,44,46,47,50,59,60]. This is related to

the excitation of higher anti-symmetric modes due to SVEGM. Currently, it is not clear how systematic this excitation is and its degree of correlation with potential detrimental effects of asynchronous motion.

Given the above lack of clarity, it is not surprising that most seismic codes worldwide do not address the above issue. In fact, with very few exceptions, they do not even recommend a solid approach to generate spatially variable ground motion suites. The way in which they try to approach the problem is mainly through indirect measures, such as larger seating deck lengths and simplified methods. It is only Eurocode 8 – Part 2 for bridges [63] and the New Italian Seismic Code [64] that explicitly deal with the SVEGM. However, the provisions of these codes aim at capturing solely bridges' distress due to the pseudo-static response component ignoring the potential impact of higher anti-symmetric modes' excitation. What's worse, these simplified methods have a minor effect on the predicted design quantities when compared to more sophisticated ones and, quite naturally, they are not applicable to bridges which are insensitive to statically imposed displacements, such as for instance seismically isolated ones [58]. Overall, in all cases, modern seismic codes in the U.S., Europe and Asia are very reluctant to provide a detailed framework for considering the SVEGM effect in the design and assessment of bridges. This may be attributed to the widely prevailing perception that considering asynchronous earthquake input motion has a higher level of uncertainty compared to not addressing the problem at all.

In this context, the objective of this paper is to study the effects of spatial variability of earthquake ground motion on the dynamic response of base-isolated R/C bridges, with the specific aim to quantify the excitation of anti-symmetric modes of vibration and investigate its correlation with bridge response quantities. Different scenarios of input motion are considered involving soil classes, wave propagation velocities and loss of correlation patterns among the various supports. Lumped springs and dashpots are distinctly calculated for every different foundation and excitation case to model the interacting soil-bridge system, while excitation input motions are generated using an evolutionary PSD and are EC8 spectrum-compatible. The results of this analysis are presented in the following sections.

2. PARAMETRIC ANALYSIS

2.1 Bridge response under multiple support excitation

The response of a structure with N degrees of freedom (DOF) and M supports (constrained DOF) under asynchronous input motion is given by [65]:

$$u^{total}(t) = \sum_{k=1}^{M} \{r_k\} u_{g,k}(t) + \sum_{k=1}^{M} \sum_{i=1}^{N} \Phi_i \Gamma_{i,k} D_{i,k}(t) \quad (1)$$

where the first term represents the pseudo-static component of the response and the second term the dynamic one. $\{r_k\}$, which is the k^{th} column of the N by M influence matrix, contains the displacements of the unconstrained DOF when the k^{th} support is displaced by unit while all the other supports are fixed, $u_{g,k}(t)$ is the displacement input time history at the k^{th} support, φ_i is the eigenvector of mode i, $D_{i,k}(t)$ is the response of a single d.o.f. oscillator with the dynamic characteristics of mode i, subjected to the accelerations $\ddot{u}_{g,k}(t)$, and $\Gamma_{i,k} = \varphi_i^T M\{r_k\}/\varphi_i^T M\varphi_i$ is the modal participation factor of mode i that is related to the excitation of the k^{th} support. It is important to note that in the case of a structure subjected to uniform input motion, the modal participation factor of mode i is: $\Gamma_i = \sum_{k=1}^{M} \Gamma_{i,k}$.

The motion's dynamic component is primarily affected by the contribution of the anti-symmetric modes. In this case, factors $\Gamma_{i,k}$ for k=1,2,…M have different signs and therefore, under uniform excitation, they are either cancelled out or their sum is small enough to result in a minor contribution of anti-symmetric mode *i* to the total response. However, this is not valid when asynchronous input motion is considered with the effects of anti-symmetric modes' contribution observed locally at the regions where the maximum values of their eigenvectors take place. This is quite interesting, especially in case of bridges where the deck rests on the piers through elastomeric bearings, since such structures are insensitive to statically imposed displacements.

2.2. Overview

A parametric analysis was conducted to investigate the modified dynamic response of a real bridge and the respective excitation of its anti-symmetric modes due to SVEGM. Lissos Bridge was selected as the case study parametrically varying apparent propagation velocity of seismic waves (V_{app}= 500, 1000, 1500 m/s), soil class according to EC8 (A, B, C, D), peak ground acceleration PGA (0.16g, 0.24g, 0.36g- values adopted in the National EC8 Annex for Greece) and the loss of coherency as summarised in Table 1. The latter strongly depends on the coherency model used [66]; however, such an examination goes beyond the scope of the present study. Similarly to Saxena, Deodatis, and Shinozuka [45] twenty sample functions of input motion sets were generated for each combination using the method of Cacciola & Deodatis [28], which is based on the spectral representation technique. The effects of asynchronous excitation were investigated with the use of a foundation element model which accounts for soil-structure-interaction by introducing appropriate dynamic impedances for each soil and excitation pair. Calculating the Fourier

amplitude spectra of the accelerations at the deck over each pier, excitation of the anti-symmetric modes was investigated and subsequently correlated with the effects of SVEGM on the drift and bending moments of the bridge piers.

Table 1: The scenarios examined. Twenty realizations (multivariate vectors) were produced for each case.

Soil	V_{app} [m/s]	0.16[g]		0.24[g]		0.36[g]	
		Coherency		Coherency		Coherency	
		Without	With	Without	With	Without	With
*	500	*-16-5-N	*-16-5-Y	*-24-5-N	*-24-5-Y	*-36-5-Y	*-36-5-Y
	1000	*-16-10-N	*-16-10-Y	*-24-10-N	*-24-10-Y	*-36-10-Y	*-36-10-Y
	1500	*-16-15-N	*-16-15-Y	*-24-15-N	*-24-15-Y	*-36-15-Y	*-36-15-Y
* denotes any soil class A, B, C or D as described in EC8							

2.3. The Lissos Bridge

The Lissos River road bridge is an 11-span, base-isolated, R/C structure of an overall length of 433m, located along the Egnatia Highway in northeastern Greece [67]. It consists of two independent branches. The deck is a continuous, single-cell, pre-stressed concrete box of a constant depth of 2.75m and 14.25m wide (concrete class: B35 (kg/cm^2), reinforcing steel class: St420/500, pre-stressing steel class: St1570/1770), that rests through elastomeric bearings on 10 piers, and through roller bearings (450x600x55.5, movement capacity +265mm/-365mm) on the abutments, where expansion joints (≥330mm) exist. The transverse displacement of the deck over each pier is restricted to 10cm by stoppers of 1.20m height, while it is entirely prevented at the abutments through lateral elastomeric bearings. The piers are made of reinforced concrete (class B35, reinforcing steel class: St420/500) and their heights vary between 4.50m to 10.50m. Figure 1 illustrates the cross sections of the piers and the deck.

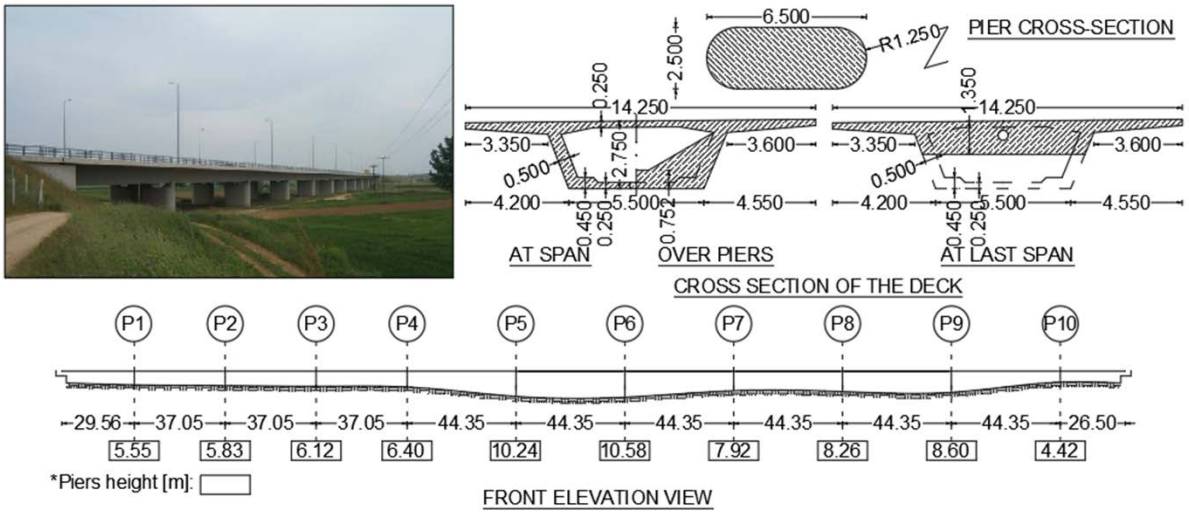

Figure 1: The Lissos River road bridge and its cross sections.

The bridge was selected as a test-bed for the problem at hand because (a) it is long enough to be reasonably sensitive (on the basis of both research findings and EC8 criteria) to spatial variability of ground motion, (b) due to the large number of piers entailed, which are expected to generate a statistically adequate sample of response quantities, and (c) given that base-isolated bridges have been specifically identified as a case where the current provisions of EC8 are not applicable.

3. GENERATION OF SPATIALLY VARIABLE INPUT MOTION

The method proposed by Cacciola & Deodatis [28] is used herein for the generation of *m*-variate, fully non-stationary, spectrum-compatible ground motion vector processes. This method considers the simulated ground motion vector process $f_j^{SC}(t)$ as the superposition of two other processes $f_j^{SC}(t) = f_j^{L}(t) + f_j^{C}(t)$: (a) a fully non-stationary process $f_j^{L}(t)$, with known cross-spectral density matrix $S^{L}(\omega,t)$ that represents the desired geological and seismological conditions, and (b) a quasi-stationary corrective process $f_j^{C}(t)$, the cross-spectral density of which $S^{C}(\omega)$ has to be determined so as the simulated motions to be spectrum-compatible. More specifically, the method initiates with the definition of (a) the target response spectra $RSA^{(j)}$ at each location *j*, and (b) the evolutionary cross-spectral density matrix of the "known" $f_j^{L}(t)$ process. Using one of the available methodologies provided in the literature (e.g. [19]), a pertinent representation of the fully non-stationary process $f_j^{L}(t)$ is obtained. If the averaged simulated response spectra at each location *j* are not spectrum compatible, they are scaled by 'α_j' so as to match the respective targeted response spectrum at least at one frequency, with all the other spectral values remaining lower than

the targeted ones. Then, the PSD function of the corrective process $G^C(\omega)$ ($=2\,S^C(\omega)$, $\omega \geq 0$; $=0$ elsewhere) is calculated through a recursive procedure as follows:

$$G_j^C\left(\omega_i\right) = 0, \quad 0 \leq \omega \leq \omega_{lc} \tag{2}$$

$$G_j^C\left(\omega_i\right) = \frac{4\zeta_o}{\omega_i \pi - 4\zeta_o \omega_{i-1}} \left(\frac{\left(RSA^{(j)}\left(\omega_i, \zeta_o\right)\right)^2 - \left(RSA^{\left(f_j^L\right)}\left(\omega_i, \zeta_o\right)\right)^2}{\left(n_{U^C}^{(j)}\left(\omega_i, \zeta_0, T_S, p = 0.5\right)\right)^2} - \Delta\omega \sum_{r=1}^{i-1} G_j^C\left(\omega_r\right) \right), \; \omega_{lc} \leq \omega \leq \omega_c \frac{1}{2} \tag{3}$$

where:

$$n_{U^C}^{(j)}\left(\omega_i, \zeta_0, T_S, p = 0.5\right) = \sqrt{2\ln\left\{2N_{U^C}^{(j)}\left[1 - \exp\left[-\left(\delta_{U^C}^{(j)}\right)^{1.2}\sqrt{\pi \ln\left(2N_{U^C}^{(j)}\right)}\right]\right]\right\}} \tag{4}$$

$$N_{U^C}^{(j)} = \frac{T_S}{2\pi}\omega_i\left(-\ln p\right)^{-1} \qquad \textit{and} \qquad \delta_{UC}^{(j)} = \left[1 - \frac{1}{1-\zeta_o^2}\left(1 - \frac{2}{\pi}\arctan\frac{\zeta_o}{\sqrt{1-\zeta_o^2}}\right)^2\right]^{0.5} \tag{5}$$

$RSA^{\left(f_j^L\right)}$ is the scaled response spectrum of the fully non-stationary process $f_j^L(t)$ at location j, ζ_o is the damping ratio and T_s is the duration of strong motion which is determined through the extension of the Husid function to the stochastic processes:

$$E_L^{(j)}\left(t\right) = \frac{\int_0^t \int_0^\infty S_{jj}^L\left(\omega, t\right) d\omega dt}{\int_0^{t_f} \int_0^\infty S_{jj}^L\left(\omega, t\right) d\omega dt} \tag{6}$$

The power spectral density function $G^C(\omega)$ is then further improved through an iterative procedure:

$$G_j^C\left(\omega\right)\Big|_k = G_j^C\left(\omega\right)\Big|_{k-1}\left[\frac{\left(RSA^{(j)}\left(\omega_i, \zeta_o\right)\right)^2}{\left(RSA^{\left(f_j^L\right)}\left(\omega_i, \zeta_o\right)\right)^2 + \left(RSA^{\left(f_j^C\right)}\left(\omega_i, \zeta_o\right)\right)^2\Big|_{k-1}}\right] \tag{7}$$

until the response spectra of the simulated time histories

$$RSA^{\left(f_j^{SC}\right)}\left(\omega\right) = \sqrt{\left[RSA^{\left(f_j^L\right)}\left(\omega\right)\right]^2 + \left[RSA^{\left(f_j^C\right)}\left(\omega\right)\right]^2} \tag{8}$$

match the targeted spectra according to the desired criteria. The response spectrum $RSA^{(f_j^C)}$ is approximately calculated by the first crossing problem:

$$RSA^{\left(f_j^C\right)}\left(\omega_i\right) = \omega_i^2 n_{U^C}^{(j)}\left(\omega_i, \zeta_0, T_S, p = 0.5\right)\sqrt{\int_0^\infty \left|H\left(\omega_i, \omega\right)\right|^2 G_j^C\left(\omega\right) d\omega} \tag{9}$$

where $H(\omega_i,\omega)$ is the energy transfer function. After determining the power spectrum density $S^C(\omega)$ of the quasi-stationary corrective process $f_j^C(t)$, the evolutionary power spectrum of the simulated motions is given by:

$$S_{jj}^{SC}\left(\omega, t\right) = a_j^2 S_{jj}^{L}\left(\omega, t\right) + \varphi_j^2\left(t\right) S_{jj}^{C}\left(\omega\right) \tag{10}$$

$$S_{jk}^{SC}\left(\omega, t\right) = \sqrt{S_{jj}^{SC}\left(\omega, t\right) S_{kk}^{SC}\left(\omega, t\right)}\Gamma_{jk}\left(\omega\right) \tag{11}$$

where $\varphi(t)$ is the selected modulating function and $\Gamma_{jk}(\omega)$ is the selected coherency model. The ground motion sample functions at different locations are generated through the procedure proposed by Deodatis [19]:

$$f_j\left(t\right) = 2\sum_{r=1}^{m}\sum_{s=1}^{N}\left|H_{jr}\left(\omega_s, t\right)\right|\sqrt{\Delta\omega}\cos\left[\omega_s t - \arctan\left(\frac{\mathrm{Im}\left[H_{jr}\left(\omega_s, t\right)\right]}{\mathrm{Re}\left[H_{jr}\left(\omega_s, t\right)\right]}\right) + \varphi_{rs}\right] \tag{12}$$

where $H_{jr}(\omega_s,t)$ is the lower triangle of the Cholesky decomposition of the evolutionary power spectrum $S^{SC}(\omega,t)$ and φ_{rs} is an independent phase angle distributed uniformly within $[0,2\pi]$.

4. MODELING AND ANALYSIS

4.1. Soil and foundation of the piers

To account for soil-bridge interaction, the dynamic impedance at the foundation-soil interface is calculated. Soil class and PGA effective determine the foundation type for each different pier which was individually designed according to EC8 and EC7. The assumed soil properties for each soil class are summarized in Table 2, while the foundation for each combination of soil and PGA are presented in Table 3. Equivalently reduced shear modulus of the soil was considered as a function of PGA and the expected level of soil strain (Table 2).

Table 2: Soil properties.

Soil Class	V_s [m/s]	N_{spt}	φ^o	C [kPa]	γ [kN/m^3]	ν	β [%]	G [MPa]	G/G_{max}
B	500	60	43	0	22	0.4	3.0	550.00	0.75
C	250	30	36	15	19	0.4	3.5	118.75	0.45
D	100	10	30	8	16	0.4	4.0	16.00	0.25

Table 3: Alternative foundation design of piers for different combinations of soil stiffness and ground motion intensity.

Soil Class	PGA	Pier 1	Pier 2	Pier 3	Pier 4	Pier 5	Pier 6	Pier 7	Pier 8	Pier 9	Pier 10
A		All piers are fixed									
B	0.16	Spread footing foundation (S.F.F.) 3.5/7.5									
	0.24	S.F.F. 3.5/7.5									
	0.36	S.F.F. 5.0/7.5				2x5/16			S.F.F. 5.0/7.5		
C	0.16	S.F.F. 3.5/7.5									
	0.24	S.F.F. 5.0/7.5									
	0.36	2x4/10		2x4/15		2x5/19			2x4/15		2x4/10
D	0.16	2x4/10		2x4/15		2x5/19			2x4/15		2x4/10
	0.24	2x4/10		2x4/15		2x5/19			2x4/15		2x4/10
	0.36	2x4/12		2x4/16		2x5/28		2x5/22		2x5/16	2x4/12
*For spread footing foundation: S.F.F. length X/length Y while for pile group foundation: n_x x n_y/length											

4.2. Numerical analysis

A finite element model of the Lissos Bridge was developed in SAP2000 [68] (Figure 2). Beam elements were used to simulate the piers, the deck and the stoppers, while the low damping rubber (i.e., elastomeric) bearings, were modeled using link elements with equivalent linear properties at secant stiffness. Link elements were also used to simulate the gap between the deck and the stoppers; however, due to the fact that this study investigates the anti-symmetric mode excitation of the bridge under SVEGM only, gaps were considered to be inactive (the gap opening was considered infinite) in order to exclude geometrical non-linearities due to pounding. The dynamic soil-bridge interaction was modeled using 6DOF link elements with stiffness and damping matrices reflecting the dynamic impedances of each different foundation type as calculated in Table 2, namely (a) spread footing foundations [69], or (b) pile group foundation [70,71]. Given that the dynamic stiffness and damping at the soil-foundation interface are frequency-dependent, the mean period of each input motion was used for defining the spring and dashpot properties thus accounting for the dominant frequency of each ground motion used. More refined lumped-parameter models have also been developed by the authors [72–74] that match the target impedance function along the entire frequency range in the framework of response history analysis, however, this was deemed out of scope of the particular study.

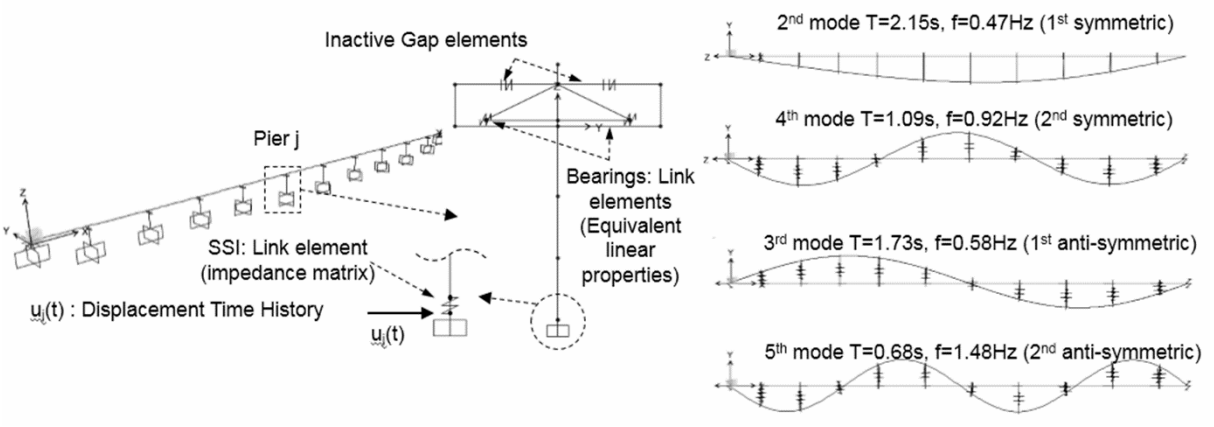

Figure 2: The finite element model of the Lissos Bridge and the first four transverse eigenmodes for the case of soil A.

At the abutments, the deck was assumed pinned along the transverse direction and free to slide in the longitudinal one. It is important to mention that different finite element models were developed for each combination of earthquake sample function, soil and PGA; this is due to the different foundation types of the piers, dynamic impedance and the mean excitation frequency of each support. Due to the aforementioned broad range of dynamic characteristics of different finite element models, Figure 2 only illustrates the first four transverse eigenmodes for the simplest case of soil A which essentially corresponds to fixed boundary conditions. The multi-support excitation was applied to the bridge as displacement time histories that have been calculated from the respective synthetic accelerograms; the latter were subjected to the necessary baseline correction using the appropriate second order polynomial for each case.

4.3. Generation of input motion

Following the process described in Section 3 for the generation of multi-variate, fully non-stationary, spectrum-compatible vector processes, a pertinent representation of the 'known' fully non-stationary component was initially obtained using the method of Deodatis [19]. The Clough & Penzien [75] acceleration power spectrum was selected to represent the cross spectral matrix of the "known" fully non-stationary process:

$$S_{jj}^{L}(\omega,t)=A(t)^{2}\,S_{o}\,\frac{\left(1+4\zeta_{g}^{2}(t)\left(\frac{\omega}{\omega_{g}(t)}\right)^{2}\right)}{\left(1-\left(\frac{\omega}{\omega_{g}(t)}\right)^{2}\right)^{2}+4\zeta_{g}^{2}(t)\left(\frac{\omega}{\omega_{g}(t)}\right)^{2}}\,\frac{\left(\frac{\omega}{\omega_{f}(t)}\right)^{4}}{\left(1-\left(\frac{\omega}{\omega_{f}(t)}\right)^{2}\right)^{2}+4\zeta_{f}^{2}(t)\left(\frac{\omega}{\omega_{f}(t)}\right)^{2}} \tag{13}$$

where $\omega_g(t)$, $\zeta_g(t)$ are the frequency and the damping ratio of the ground at point *j*, while $\omega_f(t)$ and $\zeta_f(t)$ are the respective filtering parameters. The acceleration intensity used is given by [28]:

$$S_0(t) = \frac{\sigma^2}{\pi\omega_g(t)\left(2\zeta_g(t) + \frac{1}{2\zeta_g(t)}\right)} \tag{14}$$

while the Bogdanoff-Goldberg-Bernard modulating function $A(t)=a_1te^{(-a2t)}$was utilized. The values of these variables were considered to be equal to the ones used by Cacciola & Deodatis [28], i.e. the standard deviation of the Kanai-Tajimi part of the spectrum σ=100cm/s^2, $\omega_g(t)$=20-7t/30 rad/s, $\zeta_g(t)$= 0.6-0.2t/30 rad/s, $\omega_f(t)$=0.10$\omega_g(t)$ and $\zeta_f(t)$= $\zeta_g(t)$. The Harichandran & Vanmarcke coherency model [3] (Figure 3), was selected for this study, with use of the parameters estimated by Harichandran & Wang [76] when they analyzed the data of the SMART-1 array: A=0.606, α=0.222, k=19700m, ω_o=12.692 rad/s and b=3.47:

$$\gamma_{jk}(\omega) = A\exp\left[-\frac{2\xi_{jk}}{a\theta(\omega)}(1-A-aA)\right] + (1-A)\exp\left[-\frac{2\xi_{jk}}{a\theta(\omega)}(1-A+aA)\right] \tag{15}$$

$$\theta(\omega) = k\left[1+\left(\frac{\omega}{\omega_o}\right)^b\right]^{-0.5} \tag{16}$$

The Harichandran & Vanmarcke coherency model is adopted on account of not exhibiting a sharp exponential decay with separation distance and frequency. As such, it expected to lead to higher contribution of the dynamic component in the total response of the bridge which is desirable given that the latter has been shown to dominate the response of flexible and seismically isolated bridges [77,78]. It is also noted that the use of the particular, and in fact of any other model from the literature, is quite subjective given that the seismotectonic environment of the Lissos bridge does not necessarily match that of the sites wherein the empirical or semi-empirical models were developed [66]. As a result, the use of the above coherency model is solely made for the purposes of comparison with the work of Cacciola & Deodatis [28].

The upper cut-off frequency ω_u for the simulation of the pertinent representation of the "known" vector process $f_j^I(t)$, was considered equal to 125.66 rad/s (=20Hz) and the frequency step was defined as $\Delta\omega = \omega_u/N$, where N=1048. Simulation of time histories was performed at 2048 time instances with a time step equal to 0.01s.

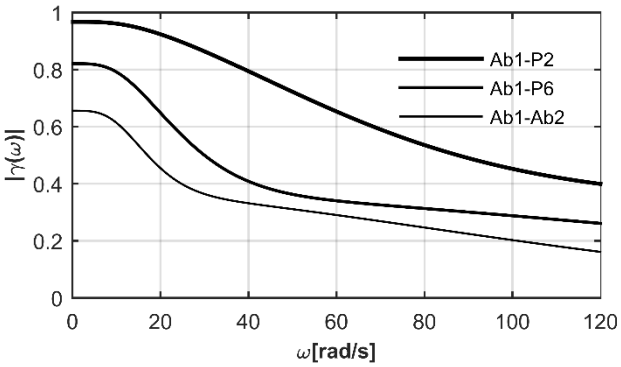

Figure 3: Harichandran & Vanmarcke loss of coherency between the signals of stations Ab1-P1 (66.61m), Ab1-P6 (229.41m) and Ab1-Ab2 (433.31m).

Having obtained a pertinent representation of the "known" vector process, the averaged simulated response spectra at each location *j* were calculated and compared with the targeted ones. The target spectra were the elastic response spectra of Type 1 provided by EC8 for soil classes A, B, C or D with respect to the examined case. Then, the recursive procedure for the estimation of the power spectral density function of the corrective process was performed. In order for the final evolutionary power spectrum to be determined, the modulating function $\varphi(t)$ (c.f. equation 10) proposed by Jennings, Housner and Tsai [79] was used:

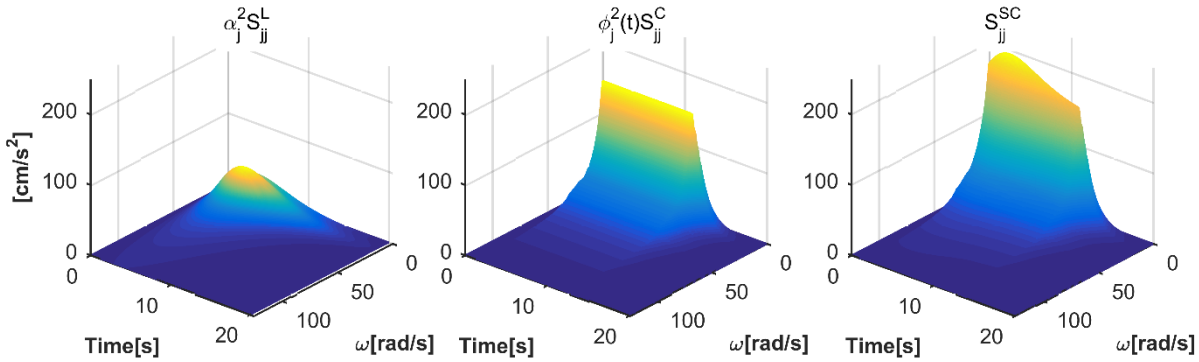

Figure 4: Scaled cross spectral matrix $S^{L}(\omega,t)$ of the "known" process $f_j(t)$ (left), the power spectrum density $S^{C}(\omega)$ of the corrective process $f_j(t)$ (in the middle) and the final evolutionary PSD at support point P4 for the case of soil B, PGA=0.24g, V_{app}=1500m/s.

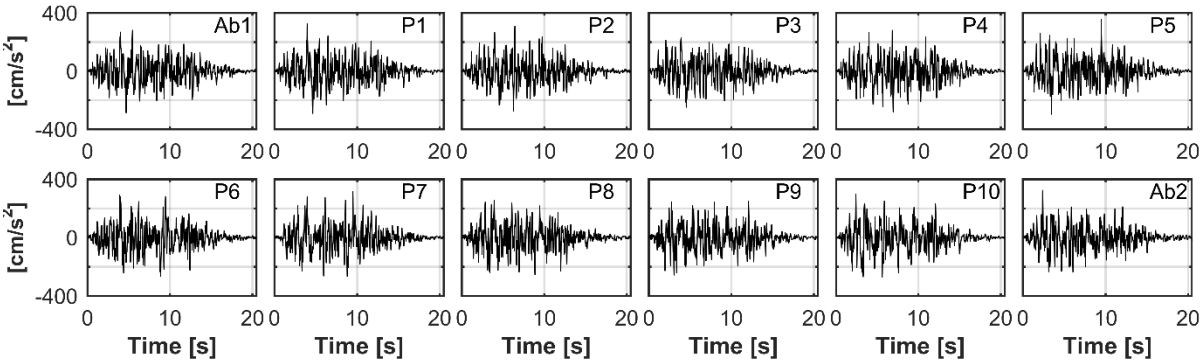

Figure 5: Typical set of accelerograms along the bridge supports for the case of soil B, PGA=0.24g, V_{app}=1500m/s.

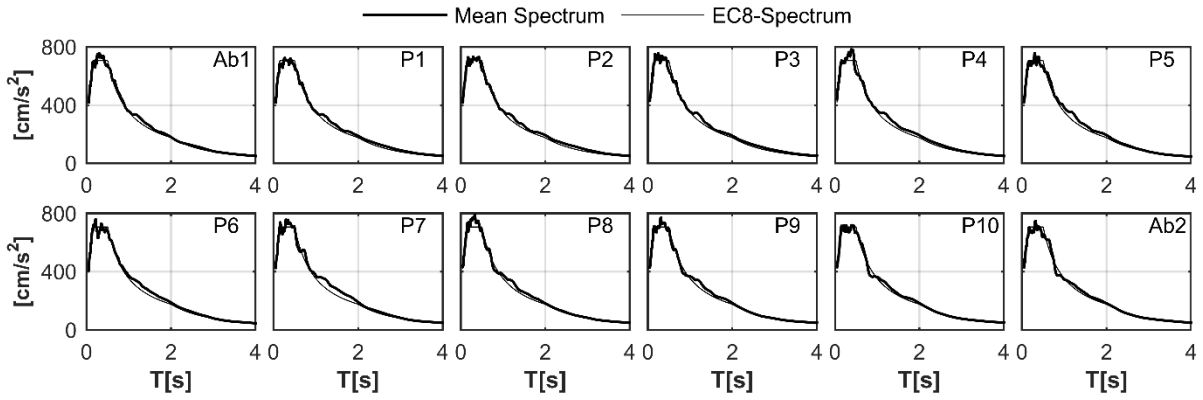

Figure 6: Comparison of the mean response spectra (20 realizations) of the generated motions for the case of soil B, PGA=0.24g, V_{app}=1500m/s with the target spectra of EC8.

$$\varphi(t)=\begin{cases}(t/t_1)^2 & t<t_1\\ 1 & t_1\le t\le t_2\\ \exp\left(-\beta(t-t_2)\right) & t>t_2\end{cases} \qquad (17)$$

where t_1 and t_2 are calculated through equation 6 and the coherency model is the same one considered at the initial stage. The scaled cross spectral matrix of the "known" process $f_j^I(t)$, the power spectral density function of the corrective process $f_j^C(t)$ and the final evolutionary PSD at support point P4 for the case of soil B, PGA=0.24g, V_{app}=1500m/s are illustrated in Figure 4.

Finally, the ground motion sample functions at different locations were generated through the procedure proposed by Deodatis, without the need for further iterations (c.f. equation 12). A typical sample function set of the accelerograms at each bridge support for the case of soil B, PGA=0.24g and V_{app}=1500m/s is illustrated in Figure 5. Convergence of the mean spectra of the

twenty sample functions generated for this combination of soil and PGA (B-0.24g) to the targeted spectra is illustrated in Figure 6.

4.4. Overview of numerical analysis

The parametric analysis performed, used artificial multi-variate, fully non-stationary, spectrum-compatible motions. In more detail, considering the loss of coherency, twenty sample functions were generated for each combination of soil class, PGA and V_{app} (Table 1), resulting in a set of 720 realizations (=4 soil classes x 3 PGA x $3V_{app}$ x 20), 12-variate, fully non-stationary, spectrum-compatible input motions. Three different cases were examined using the simulated time histories: (a) synchronous excitation due to the input motion generated at abutment (Ab_1) for each combination of soil class, PGA and V_{app}, (b) asynchronous excitation due to the finite propagation velocity V_{app} of the seismic waves using the input motion generated at abutment (Ab_1) for each combination of soil class, PGA and V_{app} (c) asynchronous excitation due to the fully-asynchronous input motion using the 720 sets of the simulated input motions. A total of 2160 analyses were performed using the direct integration method. The integration step was set to 0.005 sec.

The effects of multi-support excitation on the seismic demand are summarized on the basis of the SVEGM impact mean ratios 'ϱ'; the latter is defined as the maximum seismic demand in each pier (drift and base bending moments), calculated using differential support ground motion, over the respective EDPs using identical support input motion. Excitation of anti-symmetric modes under asynchronous input motion is investigated through the Fourier amplitude spectra of the accelerograms recorded at the deck over each pier. Next, conditional probabilities of SVEGM's impact on the drifts or bending moments at each pier in the case of anti-symmetric mode excitation are also presented. It is pointed out that the results obtained herein are valid for the selected bridge and further investigation is needed for the general case of bridges with very asymmetrical elevation profiles.

4.5. Criteria for quantifying the excitation of anti-symmetric modes

In order to investigate the excitation of higher modes and correlate them with the increase of response quantities, the Fourier spectra of the accelerations derived at the deck over at the location of each pier were computed and compared with the modal frequencies of the structure. For linear elastic response, the peak frequencies observed in the Fourier spectra coincide with the dynamic characteristics of the bridge. However, excitation of a specific mode due to asynchronous motion is less apparent and, as such, specific quantitative criteria need to be defined [80]. In this context, the criteria adopted herein for spotting an excited mode are the following:

(a) the Fourier amplitude at a specific modal frequency under asynchronous motion is at least 20% of the maximum Fourier amplitude observed at the entire frequency range under synchronous excitation.

(b) the Fourier amplitude at a specific modal frequency under asynchronous motion is higher than the respective one under synchronous excitation.

(c) mode *i,* corresponding to modal frequency f_i, activates at least 5% of the total mass in the transverse direction of the bridge or around its vertical axis.

A typical example for the quantification of anti-symmetric modes' excitation is illustrated in Figure 7. In this figure, the Fourier amplitude spectra of the accelerograms recorded at the deck over piers P3 and P7 when the bridge is excited by one of the realizations that correspond to the case of soil B, PGA=0.24g and V_{app}=500m/s are presented. The eigenvectors of the modes excited and their modal participating mass ratios are also illustrated. According to the criteria set, the 2nd anti-symmetric mode is not taken into account since it activates less than the 5% of the structure's total mass.

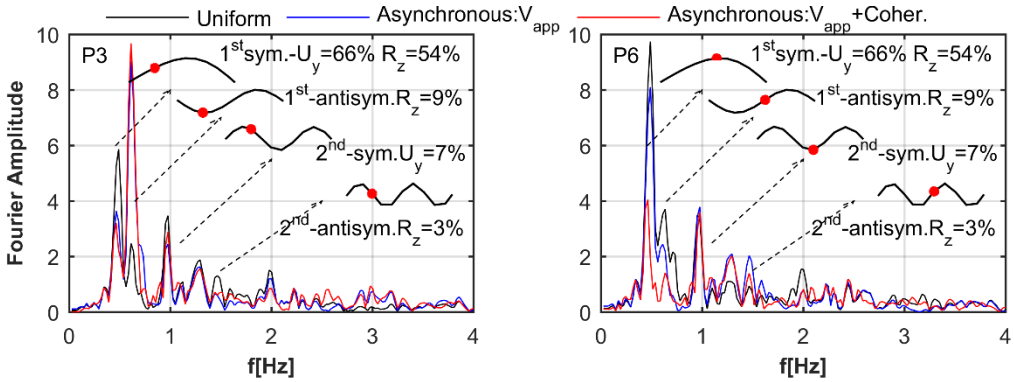

Figure 7: Fourier amplitude spectra of the accelerograms recorded at the deck over piers P3 (left) and P6 (right) under synchronous, asynchronous due to V_{app} and asynchronous due to V_{app} & Coherency input motions for the case of soil B, PGA=0.24g and V_{app}=500m/s. The first two symmetric and antisymmetric modes with their respective modal participating mass ratios are also presented.

5. RESULTS

5.1. Effects on response quantities

Given that the analyses are linear elastic and the results are expressed in the form of ratios, one would expect that the SVEGM impact ratio ϱ would be equal for different values of PGA. This is not the case though, since the input time histories were separately generated for each combination of PGA, soil and V_{app}; as a result, terms H_{jr}, θ_{jr}, and φ_{rs} in equation 12 are different for each sample

function. Consequently, the results for different values of PGA were considered to be in the same sample space for each combination of soil and V_{app}.

Figure 8 illustrates the effects of multi-support excitation on the piers' drift and bending moments for each soil class. Each line represents the mean ratio 'ϱ' of piers drift or pier base bending moments arising from 60 analyses (that is, 20 realizations x 3 PGA levels). It is seen that when only the wave passage effect is taken into account (Figure 8), SVEGM affects detrimentally only the last four piers on the right side of the bridge, assuming wave propagation from left to right, irrespectively of the soil class examined. Similar directionality has also been observed by Monti et al. [44]. Notably, these piers are located after the inflection point of the 1st anti-symmetric mode towards the direction of wave propagation. The larger the distance between a pier and the inflection point, the higher the pier's drift and moments observed due to the wave passage effect, maximum increase taking place at pier P10. To interpret this observation, two factors shall be considered: (a) the 1st antisymmetric mode is the dominant mode of vibration under asynchronous excitation forming a "node" (the term is taken from the standing waves) at the inflection point, and (b) when ground motion is assumed to propagate from left to right (i.e., from abutment A1 to A2), the time delay at point A2 is maximum. The reverse applies when the direction of excitation is taken from A2 to A1, when the maximum time delay occurs at point A1. Given that the bridge deck is continuous, this transition from the "neutral" middle node to the point of maximum delay may statistically lead to an increasing trend towards the end of the bridge, each time depending on the direction of excitation.

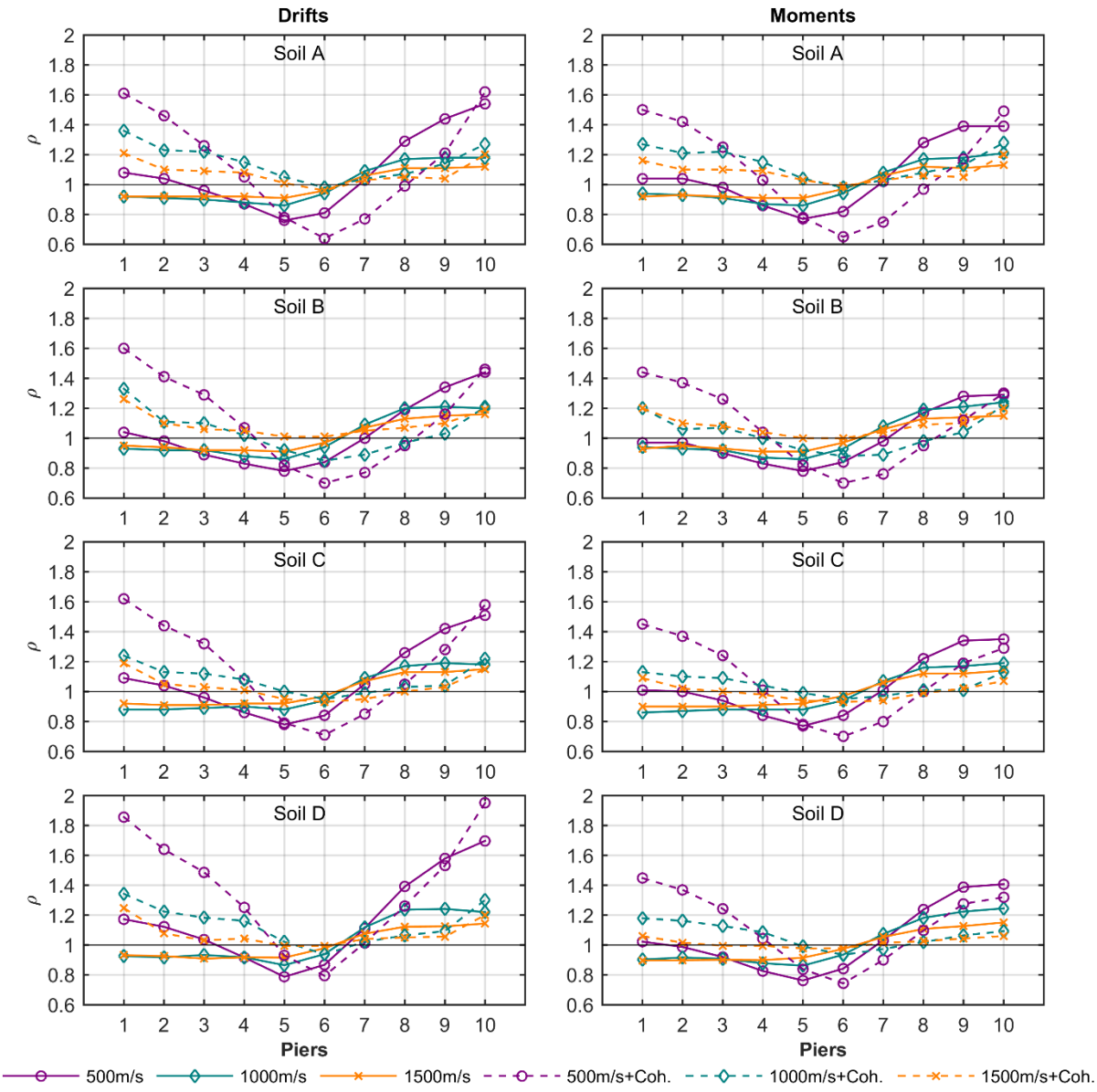

Figure 8: Mean ratios of piers' drift (left column) and bending moments (right column) under asynchronous excitation over the synchronous one for three different wave propagation velocities, with and without consideration of the loss of coherency. Each curve is the mean value of 60 analyses (3 PGA x 20 realizations).

Examining the results more closely, the increase of the drifts varies, on average, between 3-12% at pier P7, 11-39% at pier P8, 11-58% at pier P9 and 12-70% at pier P10 while the increase of bending moments on average fluctuates between 1-8% at pier P7, 11-28% at pier P8, 11-39% at pier P9 and 13-41% at pier P10. As anticipated, the lower values of these ranges correspond to the maximum V_{app}, since increasing the wave propagation velocity the ratios for all piers tend to unity and the excitations tends to uniform. On the other hand, asynchronous excitation due to finite

wave propagation velocity has a favorable effect on the piers located before the inflection point, except for the case of very low V_{app} (i.e. 500m/s).

Contrary to the case when only the wave passage effect is taken into account, when the loss of coherency is additionally considered, the detrimental effects of the SVEGM are observed to all piers except for pier P6, irrespectively of the soil class examined (Figure 8). Interestingly, this pier corresponds to the inflection point of bridge's first anti-symmetric mode, while the detrimental effects are almost symmetric with respect to this point. The larger the distance between a pier and the inflection point, the higher the pier's drift and moments observed due to SVEGM. More specifically, with respect to the examined case (soil, V_{app}), the increase of the drifts varies, on average, between 19-86% at pier P1, 5-64% at pier P2, 3-49% at pier P3, 1-25% at pier P4, 1-5% at pier P5, 1-5% at pier P7, 3-26% at pier P8, 3-53% at pier P9 and 15-95% at pier P10. Similarly, the increase of bending moments on average fluctuate between 6-50% at pier P1, 2-42% at pier P2, 7-26% at pier P3, 1-15% at pier P4, 3-4% at pier P5, 1-4% at pier P7, 1-10% at pier P8, 1-28% at pier P9 and 6-49% at pier P10. It is important to mention that, when loss of coherency is taken into account, ratios 'ϱ' of the drifts and the bending moments for piers P7, P8 and P9 are less than their respective values in the case when only the wave passage effect is considered (the continuous lines are below the dashed ones).

It is noted herein that because the presence of stoppers restraining excessive lateral displacements has not been modelled, the above increase in drift ratios for the case of asynchronous excitation consist an upper bound and may not be actually reached. To explore further this aspect, an additional set of analyses was undertaken, duly modeling the gaps and stoppers in the transverse direction under synchronous and asynchronous motion. It was observed that, indeed, the increase of the drift ratios due to asynchronous excitation was in that case lower and only up to 5% due to lateral restraint that prevented excessive movements. On the other hand, as Figure 9 below reveals, asynchronous motion has also lead to several cases where the closure of the gaps was more frequent (i.e., the pounding on the stoppers occurred more often) compared to the reference uniform excitation case. One could claim that still, the majority of the results show that the number of impacts on the stopper was either the same or lower, hence, asynchronous motion was not, at least on average, critical. This is partially true, because the favorable or neutral cases of stopper activation also may include cases where the gap does not close but the lateral displacement is increased due to asynchronous motion, thus yielding more probable to exhaust the gap.

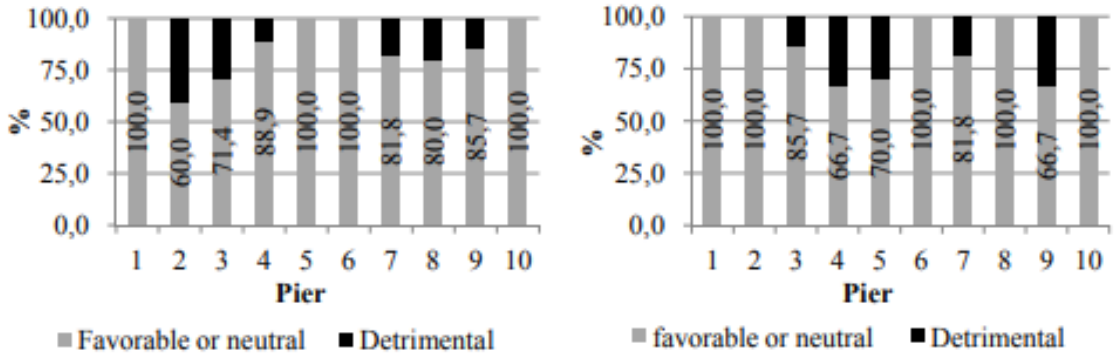

Figure 9: Effect of asynchronous excitation on the activation of stoppers in both sides of the bridge axis. Time delay effect only, V_{app} = 1500m/sec. Results from 12 realizations.

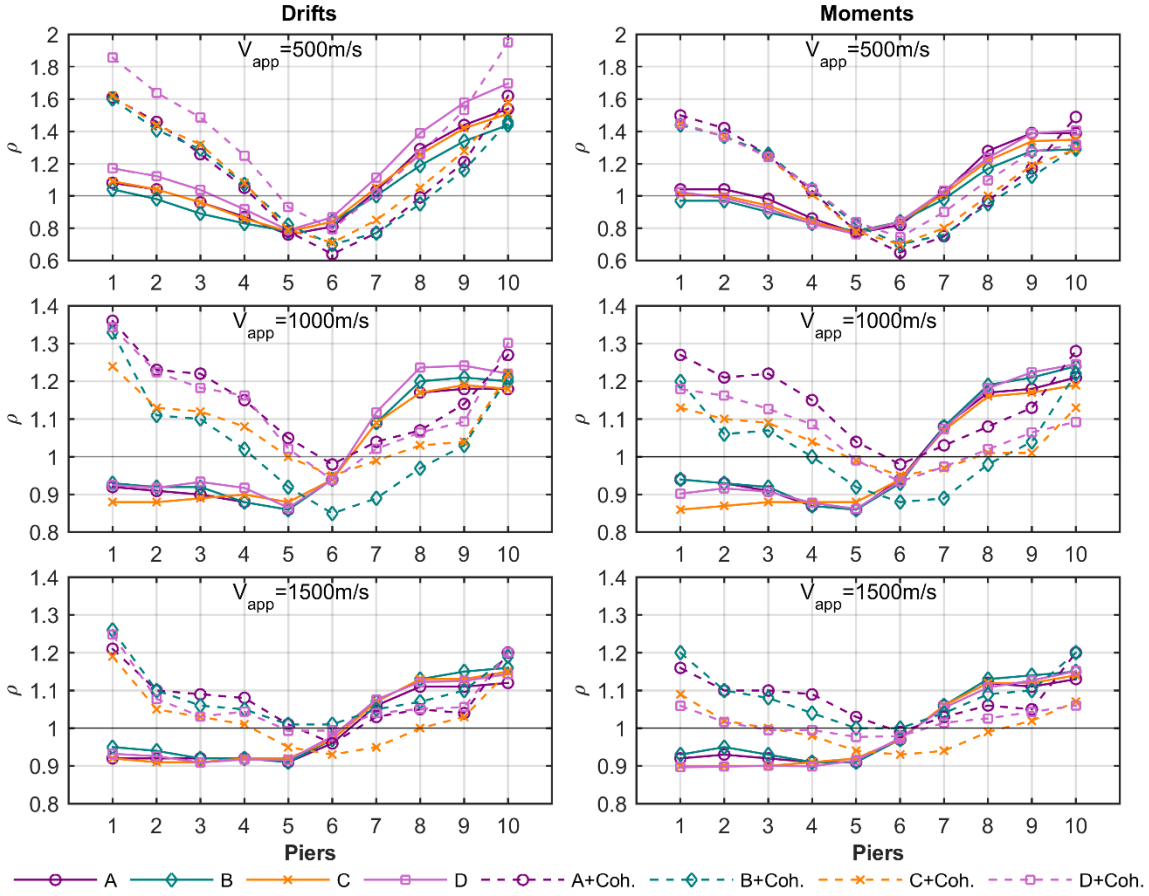

Figure 10: Effect of soil class on the mean ratios of the piers drift (left column) and bending moments (right column) under asynchronous excitation over the synchronous one for three different wave propagation velocities, with and without consideration of the loss of coherency. Each curve is the mean value of 60 analyses (3 PGA x 20 realizations).

There is therefore a combination of unfavorable effects of asynchronous motion that needs to be considered that involves both increased lateral displacements *and* more frequent impact on the stoppers, thus implying higher seismic displacement demand and potential damage, respectively.

The effect of the soil class on the EDPs studied (drift and bending moments of the piers) under asynchronous excitation is depicted in Figure 10. When considering only the wave passage effect (continuous lines), it is observed that an increase in the V_{app}, tends to equalize the mean ratios 'ϱ' of all EDPs for each soil class although there are some minor differences at the piers near the abutments. This practically implies that the soil stiffness is not a crucial parameter. In contrast and more realistically, when loss of coherency is additionally taken into account (Figure 10, dashed lines) the differences between the mean ratios 'ϱ' of the piers' drift (or bending moments) for the different soils become more evident. As anticipated, the above distribution of seismic demand cannot be reproduced or predicted assuming uniform excitation.

5.2. Anti-symmetric mode excitation and correlation to the EDPs of interest

Figure 11 illustrates the relation of the SVEGM impact ratio 'ϱ' with the excitation of higher modes for the case of soil class B, and for each pair of V_{app}, PGA, with and without considering coherency loss. To denote the case that an anti-symmetric mode is excited a red symbol is used in contrast to the case where the excitation criteria of Section 4.5 are not fulfilled, where the symbol remains green. It is seen that when an anti-symmetric mode is excited, the response quantities maybe indeed increase or decrease (ratios of ϱ>1 and ϱ<1, respectively). However, for more than 90% of the cases of detrimental effect of spatial variability (ϱ>1), this can be attributed to the excitation of a higher mode and for this very reason, the majority of the piers which experience increase of their seismic demand are located away from the point of inflection of the excited mode (i.e., P6). Given the importance of this observation, the conditional probabilities of increased seismic demand given that an anti-symmetric mode is excited, are derived as:

$$P(\rho_{Drifts/Moments} > 1 | anti-sym.mode\,excit.) = \frac{P\left(\rho_{Drifts/Moments} > 1 \cap anti-sym.mode\,excit.\right)}{P\left(anti-sym.mode\,excit.\right)} \quad (18)$$

It is seen in Figure 12 that when the wave passage effect is only considered (cases of V_{app}= 500, 1000 and 1500m/sec, solid lines, grey in B&W) the conditional probability of detrimental effects on the EDPs of interest given that an anti-symmetric mode is excited, is 0% for piers P5 and P6, thus verifying that it is not probable for spatial variability of ground motion to increase seismic demand to piers that are close to the point of inflection of the mode excited. In this case, piers P5 and P6 remain practically insensitive to the wave passage effects and the subsequent arrival of the (otherwise identical signal). On the contrary but for the same reason of mode excitation, eccentric piers such as P8-P10 have more than 90% probability to experience higher seismic demand. As for the first four piers, in the case of V_{app}=1000-1500m/sec, the conditional probability varies between

20-40% (increased demand is quite probable), while in the case of V_{app}=500m/sec, it increases up to 73% for soil class D (Figure 11 bottom).

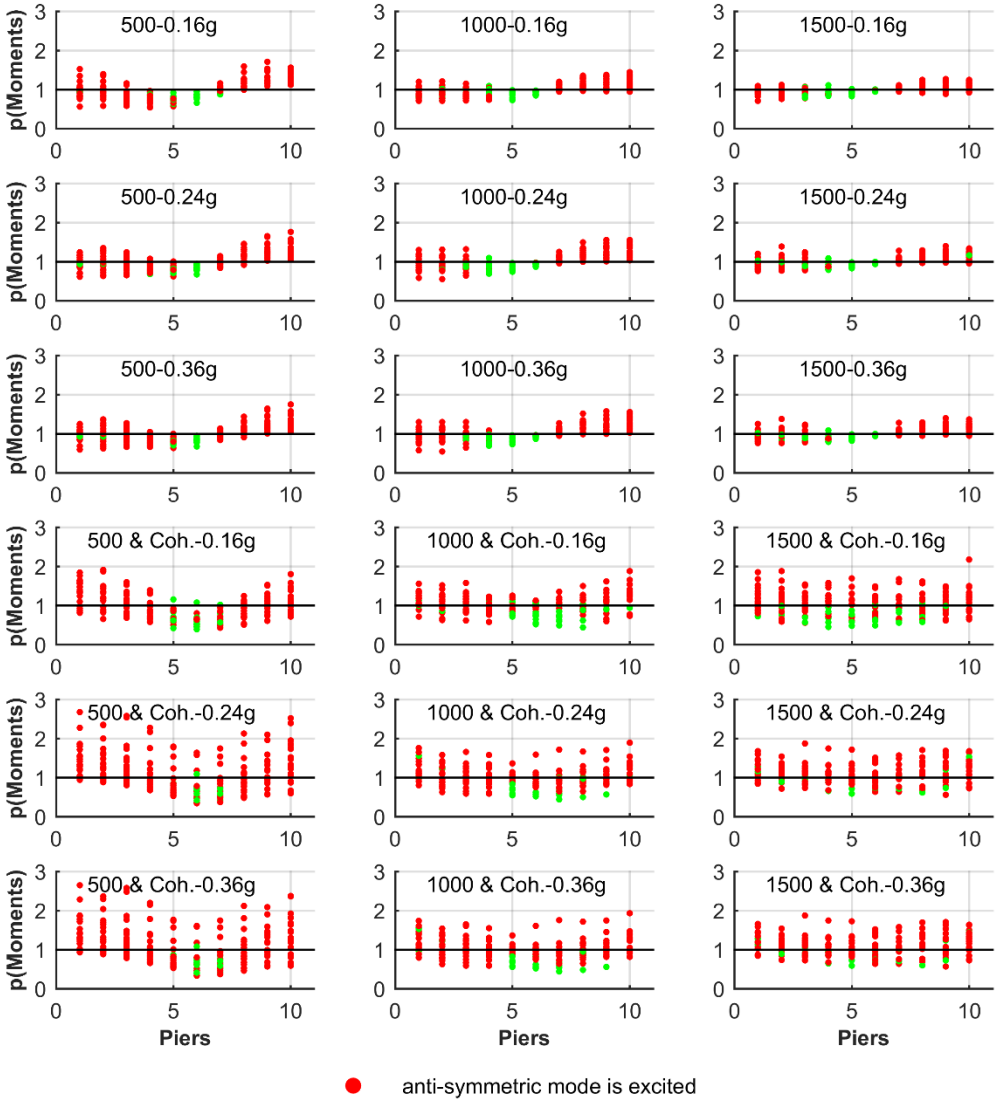

Figure 11: Ratios of seismic bending moments under asynchronous over synchronous excitation for the case of Soil B and different apparent velocities (V_{app}=500m/sec, left, V_{app}=1000m/sec middle, V_{app}=1500m/sec, right). Results of 20 realizations per pier.

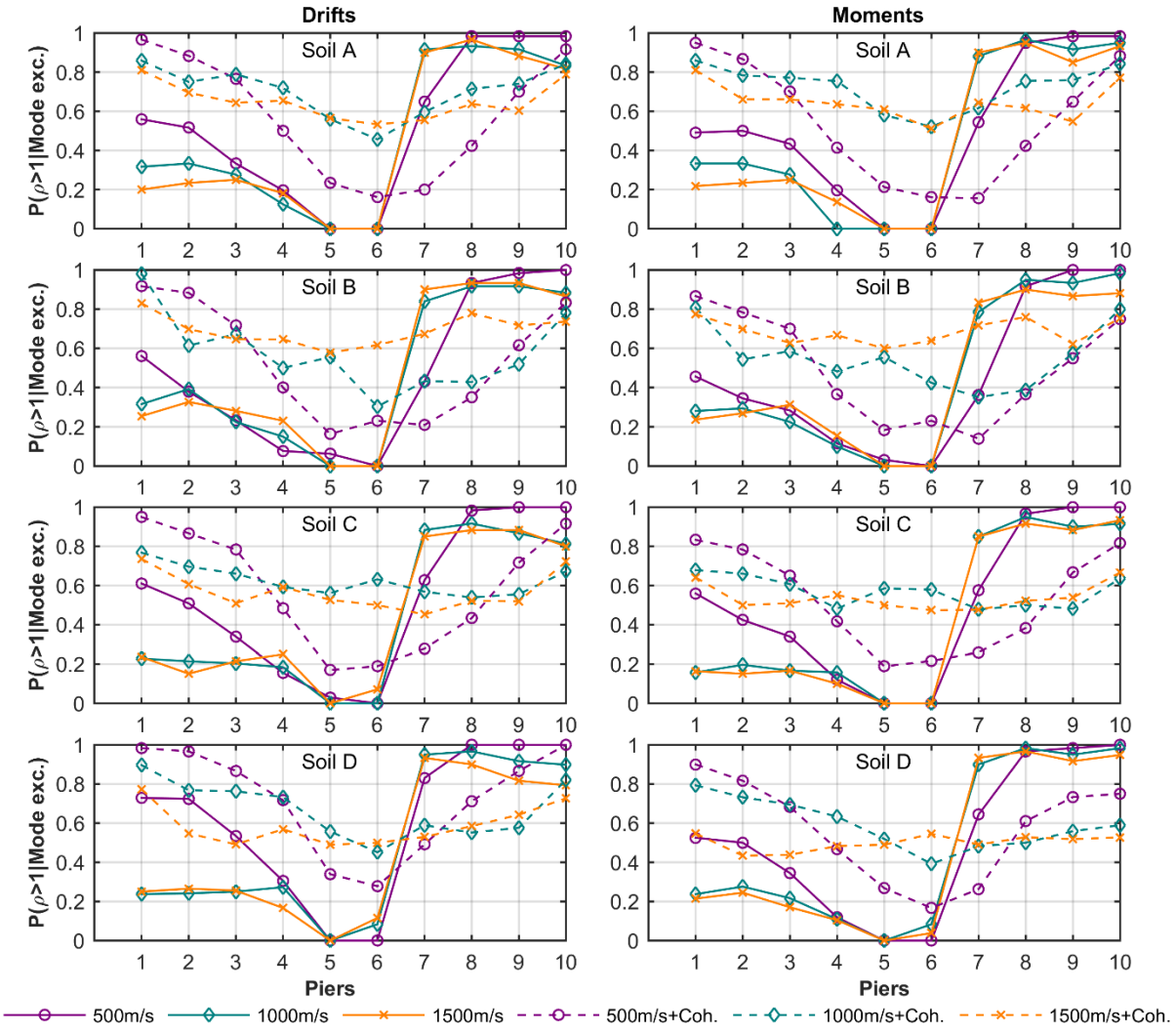

Figure 12: Conditional probabilities of increased seismic demand under multi-support excitation given that an anti-symmetric mode is excited. Soil Class variation A (top) to D (bottom).

When loss of coherency is additionally considered (cases 500m/sec+Coh, 1000m/sec+Coh, 1500m/sec+Coh), the probability that the excitation of an anti-symmetric mode will result in detrimental effects at the first six piers increases considerably. The main difference is observed in the central piers P5-P6; in the case of V_{app}=1000-1500m/s, the conditional probability at these piers is about 60%, while it is about 20% for V_{app}=500m/s. As for the conditional probability at the first four piers, it increases to more than 50%, irrespectively of the examined case. Overall, in the more realistic case of a combination of wave passage and incoherency effects, the probability of detrimental impact of SVEGM, given the excitation of a higher anti-symmetric mode of vibration is significant (typically above 50%) and tends to be more uniform even though it generally retains the main characteristic of less sensitive middle piers and more critically affected edge piers.

6. CONCLUSIONS

This paper investigates the potential effect of asynchronous excitation on the transverse-direction seismic response of base-isolated bridges with focus on the case of Lissos bridge. The reason for studying base-isolated structures to spatially variable ground motion scenarios is their insensitivity to the pseudo-static deformations that is the basis of the simplified EC8 approach for addressing this problem. To understand better the dynamic interplay between multiple support excitation and seismic demand, the excitation of anti-symmetric modes under spatially variable input motion was examined and statistically correlated with its impact on bridge response. The influence of multi-support excitation on the seismic demand was represented on the basis of mean ratios of the maximum engineering demand parameters (EDPs) of interest (in this case the drift and base bending moments of the piers), computed using differential support ground motion, over the respective quantities under identical support excitation. Different scenarios of ground motions were considered as per soil class, wave propagation velocity and loss of correlation between the motions at each support. Pier-, soil- and intensity-dependent dynamic impedances were calculated to model soil-bridge interaction, while the method proposed by Cacciola & Deodatis was used for the generation of m-variate, fully non-stationary, EC8 spectrum-compatible ground motion vector processes.

The conclusions of this study can be summarized as follows:

- In the idealised case that the wave passage effect is the only source of ground motion variability, the detrimental impacts of asynchronous excitation were concentrated on the edge piers located past the 1st antisymmetric mode inflection point given the assumed wave propagation direction (i.e., from Abutment A1 to A2 and vice-versa). A low value of apparent velocity V_{app} of the order of 500m/s that was maximizing the wave passage effect was required to observe an increase in the EDPs of interest of the remaining piers (i.e., those located before the 1st antisymmetric mode inflection point). This is due to the fact that for such levels of V_{app}, the seismic wavelength becomes equivalent to the bridge's length, whilst the frequency content of the motion remains constant, thus leading to a more uniform (and critical) response.
- When loss of coherency between the input signals was additionally taken into consideration, the detrimental effects were more uniformly distributed, irrespectively of the soil class examined, except for pier P6 which corresponds to the inflection point of bridge's 1st anti-symmetric mode.

- Statistical analysis of the cases in which the first anti-symmetric mode is excited, reveals that the response quantities maybe indeed increase or decrease (ratios of $\varrho>1$ and $\varrho<1$, respectively), but for the vast majority of seismic demand increase under SVEGM, an anti-symmetric mode had been excited. This is clearly reflected on the conditional probability of having a detrimental increase in seismic demand under multi-support excitation, given that an anti-symmetric mode is excited. The design implication of the above important observation is that not all piers are equally sensitive to asynchronous motion and this depends on the excitation of higher modes, the shape at least of which, is known in advance.
- When lateral stoppers and gaps are duly accounted for, the additional chance of triggering a higher number of impacts due to asynchronous excitation was observed. This implies that depending on the size of the gap between the deck and the stoppers, SVEGM may lead to higher displacement demands and/or more frequent impacts (and damage) on the stoppers.

Further research is needed to investigate the correlation between asynchronous motion and modes of vibration excitation, the optimum gap size of the stoppers that was not examined herein and the potential to introduce different seismic demand amplification factors for different structural components that are more sensitive to higher mode excitation.

ACKNOWLEDGEMENTS

The first author would like to thank the Hellenic State Scholarships Foundation (IKY) and Siemens for their support through the "Research Programs for Excellence IKY / Siemens" Grant, in the framework of the Hellenic Republic - Siemens Settlement Agreement.

REFERENCES

[1] Der Kiureghian A, Neuenhofer A. Response spectrum method for multi-support seismic excitations. Earthq Eng Struct Dyn 1992;21:713–40. doi:10.1002/eqe.4290210805.

[2] Sextos AG, Pitilakis KD, Kappos AJ. Inelastic dynamic analysis of RC bridges accounting for spatial variability of ground motion, site effects and soil-structure interaction phenomena. Part 1: Methodology and analytical tools. Earthq Eng Struct Dyn 2003;32:607–27. doi:10.1002/eqe.241.

[3] Harichandran RS, Vanmarcke EH. Stochastic Variation of Earthquake Ground Motion in Space and Time. J Eng Mech 1986;112:154–74. doi:10.1061/(ASCE)0733-9399(1986)112:2(154).

[4] Harichandran RS. Estimating the spatial variation of earthquake ground motion from dense array recordings. Struct Saf 1991;10:219–33. doi:10.1016/0167-4730(91)90016-3.

[5] Abrahamson NA, Schneider JF, Stepp JC. Empirical Spatial Coherency Functions for Application to Soil-Structure Interaction Analyses. Earthq Spectra 1991;7:1–27. doi:10.1193/1.1585610.

[6] Luco JE, Wong HL. Response of a rigid foundation to a spatially random ground motion. Earthq Eng Struct Dyn 1986;14:891–908. doi:10.1002/eqe.4290140606.

[7] Der Kiureghian A. A Coherency Model for Spatially Varying Ground Motions. Earthq Eng Struct Dyn 1996;25:99–111. doi:10.1002/(SICI)1096-9845(199601)25:1<99::AID-EQE540>3.0.CO;2-C.

[8] Zerva A, Shinozuka M. Stochastic differential ground motion. Struct Saf 1991;10:129–43. doi:10.1016/0167-4730(91)90010-7.

[9] Liao S, Li J. A stochastic approach to site-response component in seismic ground motion coherency model. Soil Dyn Earthq Eng 2002;22:813–20. doi:10.1016/S0267-7261(02)00103-3.

[10] Harichandran RS. Spatial variation of earthquake ground motion, what is it, how do we model it, and what are its engineering implications. East Lansing, MI: 1999.
[11] Liao S, Zerva A. Physically compliant, conditionally simulated spatially variable seismic ground motions for performance-based design. Earthq Eng Struct Dyn 2006;35:891–919. doi:10.1002/eqe.562.
[12] Konakli K, Der Kiureghian A. Simulation of spatially varying ground motions including incoherence, wave-passage and differential site-response effects. Earthq Eng Struct Dyn 2012;41:495–513. doi:10.1002/eqe.1141.
[13] Shinozuka M, Deodatis G. Stochastic process models for earthquake ground motion. Probabilistic Eng Mech 1988;3:114–23. doi:10.1016/0266-8920(88)90023-9.
[14] Shinozuka M, Deodatis G. Simulation of Stochastic Processes by Spectral Representation. Appl Mech Rev 1991;44:191. doi:10.1115/1.3119501.
[15] Shinozuka M. Monte Carlo solution of structural dynamics. Comput Struct 1972;2:855–74. doi:10.1016/0045-7949(72)90043-0.
[16] Yang J-N. Simulation of random envelope processes. J Sound Vib 1972;21:73–85. doi:10.1016/0022-460X(72)90207-6.
[17] Zerva A. Seismic ground motion simulations from a class of spatial variability models. Earthq Eng Struct Dyn 1992;21:351–61. doi:10.1002/eqe.4290210406.
[18] Deodatis G. Simulation of ergodic multivariate stochastic processes. J Eng Mech 1996;122:778–87. doi:10.1061/(ASCE)0733-9399(1996)122:8(778).
[19] Deodatis G. Non-stationary stochastic vector processes: seismic ground motion applications. Probabilistic Eng Mech 1996;11:149–67. doi:10.1016/0266-8920(96)00007-0.
[20] Bi K, Hao H. Modelling and simulation of spatially varying earthquake ground motions at sites with varying conditions. Probabilistic Eng Mech 2012;29:92–104. doi:10.1016/j.probengmech.2011.09.002.
[21] Shinozuka M, Deodatis G. Simulation of multi-dimensional Gaussian stochastic fields by spectral representation. Appl Mech Rev 1996;49:29–53. doi:10.1115/1.3101883.
[22] Hao H, Oliveira CS, Penzien J. Multiple-station ground motion processing and simulation based on smart-1 array data. Nucl Eng Des 1989;111:293–310. doi:10.1016/0029-5493(89)90241-0.
[23] Gao Y, Wu Y, Li D, Liu H, Zhang N. An improved approximation for the spectral representation method in the simulation of spatially varying ground motions. Probabilistic Eng Mech 2012;29:7–15. doi:10.1016/j.probengmech.2011.12.001.
[24] Lavorato D, Bergami AV, Rago C, Ma H-B, Nuti C, Vanzi I, et al. Seismic behaviour of isolated RC bridges subjected to asynchronous seismic input. Proc. 6th Int. Conf. Comput. Methods Struct. Dyn. Earthq. Eng. (COMPDYN 2015), vol. 1, Athens: Institute of Structural Analysis and Antiseismic Research School of Civil Engineering National Technical University of Athens (NTUA) Greece; 2017, p. 2214–26. doi:10.7712/120117.5561.18104.
[25] Lavorato D, Vanzi I, Nuti C, Monti G. Generation of Non-synchronous input earthquake signals. In: P G, editor. Risk Reliab. Anal. Theory Appl. Honor Prof. Armen Der Kiureghian, Springer; 2017, p. 169–82.
[26] Shields MD. Simulation of spatially correlated nonstationary response spectrum – compatible ground motion time histories. J Eng Mech 2014;141:4014161. doi:10.1061/(ASCE)EM.1943-7889.0000884.
[27] Cacciola P. A stochastic approach for generating spectrum compatible fully nonstationary earthquakes. Comput Struct 2010;88:889–901. doi:10.1016/j.compstruc.2010.04.009.
[28] Cacciola P, Deodatis G. A method for generating fully non-stationary and spectrum-compatible ground motion vector processes. Soil Dyn Earthq Eng 2011;31:351–60. doi:10.1016/j.soildyn.2010.09.003.
[29] Cacciola P, Zentner I. Generation of response-spectrum-compatible artificial earthquake accelerograms with random joint timefrequency distributions. Probabilistic Eng Mech 2012;28:52–8. doi:10.1016/j.probengmech.2011.08.004.
[30] Perotti F. Structural response to non-stationary multiple-support random excitation. Earthq Eng Struct Dyn 1990;19:513–27. doi:10.1002/eqe.4290190404.
[31] Nuti C, Vanzi I. Influence of earthquake spatial variability on differential soil displacements and SDF system response. Earthq Eng Struct Dyn 2005;34:1353–74. doi:10.1002/eqe.483.
[32] Yamamura N, Tanaka H. Response analysis of flexible MDF systems for multiple-support seismic

excitations. Earthq Eng Struct Dyn 1990;19:345–57. doi:10.1002/eqe.4290190305.
[33] Harichandran RS, Hawwari A, Sweidan BN. Response of Long-Span Bridges to Spatially Varying Ground Motion. J Struct Eng ASCE 1996;122:476–84. doi:10.1061/(ASCE)0733-9445(1996)122:5(476).
[34] Soyluk K, Dumanoglu AA. Spatial variability effects of ground motions on cable-stayed bridges. Soil Dyn Earthq Eng 2004;24:241–50. doi:10.1016/j.soildyn.2003.11.005.
[35] Lin J., Zhang Y., Li Q., Williams F. Seismic spatial effects for long-span bridges, using the pseudo excitation method. Eng Struct 2004;26:1207–16. doi:10.1016/j.engstruct.2004.03.019.
[36] Nazmy AS, Abdel-Ghaffar AM. Effects of ground motion spatial variability on the response of cable-stayed bridges. Earthq Eng Struct Dyn 1992;21:1–20. doi:10.1002/eqe.4290210101.
[37] Der Kiureghian A, Keshishian P, Halabian AM. Multiple support response spectrum analysis of bridges including the site-response effect & the MSRS code. Berkeley, CA:University of California: 1997.
[38] Trifunac MD, Todorovska MI. Response spectra for differential motion of columns. Earthq Eng Struct Dyn 1997;26:251–68. doi:10.1002/(SICI)1096-9845(199702)26:2<251::AID-EQE642>3.0.CO;2-B.
[39] Zembaty Z, Rutenberg A. Spatial reponse spectra and site amplification effects. Eng Struct 2002;24:1485–96. doi:10.1016/S0141-0296(02)00096-2.
[40] Trifunac MD, Gicev V. Response spectra for differential motion of columns paper II: Out-of-plane response. Soil Dyn Earthq Eng 2006;26:1149–60. doi:10.1016/j.soildyn.2006.05.009.
[41] Zembaty Z. Spatial seismic excitations and response spectra. ISET J Earthq Technol 2007;44:233–58.
[42] Price TE, Eberhard MO. Effects of Spatially Varying Ground Motions on Short Bridges. J Struct Eng 1998;124:948–55. doi:10.1061/(ASCE)0733-9445(1998)124:8(948).
[43] Konakli K, Der Kiureghian A. Extended MSRS rule for seismic analysis of bridges subjected to differential support motions. Earthq Eng Struct Dyn 2011;40:1315–35. doi:10.1002/eqe.1090.
[44] Monti G, Nuti C, Pinto PE. Nonlinear Response of Bridges under Multisupport Excitation. J Struct Eng 1996;122:1147–59. doi:10.1061/(ASCE)0733-9445(1996)122:10(1147).
[45] Shinozuka M, Saxena V, Deodatis G. Effect of spatial variation of ground motion on highway structures. Princeton, NJ: 2000.
[46] Tzanetos, Elnashai, Hamdan, Antoniou. Inelastic Dynamic Response of RC Bridges Subjected to Spatial Non-Synchronous Earthquake Motion. Adv Struct Eng 2000;3:191–214. doi:10.1260/1369433001502148.
[47] Burdette NJ, Elnashai AS. Effect of asynchronous earthquake motion on complex bridges. II: Results and implications on assessment. J Bridg Eng 2008:166–72.
[48] Lupoi A, Franchin P, Pinto PE, Monti G. Seismic design of bridges accounting for spatial variability of ground motion. Earthq Eng Struct Dyn 2005;34:327–48. doi:10.1002/eqe.444.
[49] Pinto P, Franchin P. Issues in the Upgrade of Italian Highway Structures. J Earthq Eng 2010;14:1221–52. doi:10.1080/13632461003649970.
[50] Sextos AG, Kappos AJ, Pitilakis KD. Inelastic dynamic analysis of RC bridges accounting for spatial variability of ground motion, site effects and soil-structure interaction phenomena. Part 2: Parametric study. Earthq Eng Struct Dyn 2003;32:629–52. doi:10.1002/eqe.242.
[51] Sextos A, Kappos AJ, Mergos P. Effect of soil-structure interaction and spatial variability of ground motion on irregular bridges: the case of the Krystallopigi bridge. Proc. 13th World Conf. Earthq. Eng., Vancouver, Canada: 2004.
[52] Burdette NJ, Elnashai AS, Lupoi A, Sextos AG. Effect of Asynchronous Earthquake Motion on Complex Bridges. I: Methodology and Input Motion. J Bridg Eng 2008;13:158–65. doi:10.1061/(ASCE)1084-0702(2008)13:2(158).
[53] Lou L, Zerva a. Effects of spatially variable ground motions on the seismic response of a skewed, multi-span, RC highway bridge. Soil Dyn Earthq Eng 2005;25:729–40. doi:10.1016/j.soildyn.2004.11.016.
[54] Monti G, Pinto PE. Effects of Multi-support excitation on isolated bridges. In: Friedland I, Constantinou. M., editors. Proc. U.S.-Italy Work. Seism. Prot. Syst. Bridg., 1998, p. 225.
[55] Zanardo G, Hao H, Modena C. Seismic response of multi-span simply supported bridges to a spatially varying earthquake ground motion. Earthq Eng Struct Dyn 2002;31:1325–45. doi:10.1002/eqe.166.

[56] Lupoi A. The Response of Isolated Bridges Accounting for Spatial Variability of Ground Motion. J Earthq Eng 2009;13:814–34. doi:10.1080/13632460802645106.
[57] Pinto PE, Franchin P. Open Issues in the Seismic Design and Assessment of Bridges. In: Garevski M, Ansal A, editors. Earthq. Eng. Eur., vol. 17, Dordrecht: Springer Netherlands; 2010, p. 568. doi:10.1007/978-90-481-9544-2.
[58] Sextos AG, Kappos AJ. Evaluation of seismic response of bridges under asynchronous excitation and comparisons with Eurocode 8-2 provisions. Bull Earthq Eng 2009;7:519–45. doi:10.1007/s10518-008-9090-5.
[59] Abdel Raheem S, Hayashikawa T, Dorka U. Spatial variation effects on seismic response control of calble-stayed bridges. 12h World Conf. Earthq. Eng., 2008, p. 1–11.
[60] Sextos AG, Karakostas C, Lekidis V, Papadopoulos S. Multiple support seismic excitation of the Evripos bridge based on free-field and on-structure recordings. Struct Infrastruct Eng 2015;11:1510–23. doi:10.1080/15732479.2014.977302.
[61] Mwafy A, Kwon O, Elnashai A, Hashash Y. Wave Passage and Ground Motion Incoherency Effects on Seismic Response of an Extended Bridge. J Bridg Eng 2011;16:364–74.
[62] Yang Z, He L, Bielak J, Zhang Y, Elgamal A, Conte J. Nonlinear seismic response of a bridge site subject to spatially varying ground motion. 16th ASCE Eng. Mech. Conf., Seattle,WA, USA: 2003.
[63] CEN. European Standard EN 1998-2. Eurocode 8: Design of structures for earthquake resistance—Part 2: Bridges. Brussels: CEN: 2005.
[64] Infrastrutture M. Norme Tecniche per le Costruzioni [Technical Standards for Construction]. Gazzetta Ufficiale della Repubblica Italiana. 29:(S.O. 30) (in Italian). Rome, Italy: Istituto Poligrafico e Zecca dello Stato; 2008.
[65] Chopra AK. Dynamics of Structures: Theory and applications to earthquake engineering. 3rd ed. Upper Saddle River, NJ: Prentice-Hall Inc; 2007.
[66] Zerva A, Zervas V. Spatial variation of seismic ground motions: An overview. Appl Mech Rev 2002;55:271. doi:10.1115/1.1458013.
[67] Stathopoulos S. Bridge Engineering in Greece. In: Chen WF, Duan L, editors. Handb. Int. Bridg. Eng., CRC Press Taylor & Francis Group; 2013.
[68] CSI. CSI analysis reference manual for SAP2000 2009.
[69] Mylonakis GE, Nikolaou S, Gazetas G. Footings under seismic loading: analysis and design issues with emphasis on bridge foundations. Soil Dyn Earthq Eng 2006;26:824–53.
[70] Gazetas G. Foundation vibrations. In: Fang H-Y, editor. Found. Eng. Handb., Springer US; 1991, p. 553–93. doi:10.1007/978-1-4757-5271-7_15.
[71] Pender M. Aseismic pile foundation design analysis. Bull New Zeal Natl Soc Earthq Eng 1993;26:49–160.
[72] Lesgidis ND, Kwon O-S, Sextos AG. A time-domain seismic SSI analysis method for inelastic bridge structures through the use of a frequency-dependent lumped parameter model. Earthq Eng Struct Dyn 2015;44:2137–56. doi:10.1002/eqe.
[73] Lesgidis ND, Sextos A, Kwon O-S. Influence of frequency-dependent soil-structure interaction on the fragility of R/C bridges. Earthq Eng Struct Dyn 2017;46:139–58. doi:10.1002/eqe.2778.
[74] Lesgidis ND, Sextos AG, Kwon O-S. A frequency- and intensity- dependent macroelement for reduced order seismic analysis of soil-structure interacting systems. Earthq Eng Struct Dymamics 2018:5–26.
[75] Clough RW, Penzien J. Dynamics of structures. Third Edit. Berkeley, CA: Computers & Structures, Inc.; 2003.
[76] Harichandran RS, Wang W. Effect of spatially varying seismic excitation on surface lifelines. 4th U.S. Natl. Conf. Earthq. Eng., Palm Springs: 1990.
[77] Zerva A. Seismic loads predicted by spatial variability models. Struct Saf 1992;11:227–43. doi:10.1016/0167-4730(92)90016-G.
[78] Zerva A, Ang A.-S, Wen YK. Development of differential response spectra for lifeline seismic analysis. Probabilistic Eng Mech 1986;1:208–18. doi:10.1016/0266-8920(86)90014-7.
[79] Jennings PC, Housner GW, Tsai NC. Simulated Earthquake Motions. 4th World Conf. Earthq. Eng., Santiago, Chile: 1969.
[80] Papadopoulos SP, Sextos AG. On the excitation of higher modes of long bridges due to spatial variability of earthquake ground motion. Innov. Bridg. Soil-Bridge Interact. (IBSBI), Athens, Greece: 2011.